Life Term Information Quantity: A Unified Informational-Thermodynamic Framework of Cosmology, Nilpotent Quantum Dynamics, and Biological Intent

The Epistemological Crisis of Continuous Realities and the EML Operator

Modern theoretical physics and mathematics face a deep conceptual crisis originating from the reliance on continuous real numbers (\mathbb{R}) as the fundamental substrate of physical laws. Historically, the continuous description of spacetime and field variables has yielded highly precise predictions. However, this continuity is increasingly recognized as a cognitive projection—a human "User Interface" that masks a discrete, informational reality.
This limitation is illustrated by the Peano Trap and the Lonely Runner Conjecture (LRC). The Lonely Runner Conjecture states that for N runners on a circular track of unit length with distinct, constant speeds, there will always be a time when every runner is "lonely" (separated from all others by a distance of at least 1/N). While this conjecture has been proven for N \le 10, standard Zermelo-Fraenkel set theory with the Axiom of Choice (ZFC) fails to provide a general proof for N \ge 11. This failure is not a simple computational bottleneck. It is a fundamental limitation of continuous mathematics, where the continuous real number system introduces unprovable infinities and undecidable topological loops.
To resolve this limitation, Andrzej Odrzywolek (2026) introduced a fundamental mathematical operator known as the EML (Exponent-Logarithm) operator :
EML(x, y) = e^x - \ln(y) + 1
The EML operator serves as the "single atom of mathematics," from which the entire landscape of fundamental constants (e, \pi, i) and elementary operations can be generated through recursive nesting. By defining numbers not as static points on a continuous line, but as discrete operations of potentiality and actuality, the EML framework bypasses the unprovable loops of ZFC. This shift allows the continuum of real numbers to be reconstructed as a discrete, binary tree structure composed of nested EML units. Consequently, physical and biological systems can be modeled without the unphysical singularities associated with continuous spacetime.

Zero Ontology, Nilpotent Algebra, and the L-Operator

The transition from a continuous ontological framework to a discrete, informational substrate requires a revision of the concept of "nothingness." Standard arithmetic relies on a destructive multiplication rule:
x \times 0 = 0
This operation is fundamentally non-invertible, representing an absolute destruction of

information that violates physical conservation laws. The L-Model resolves this "Zero Ontology" by replacing standard multiplication with a Nilpotent Algebra. Under this framework, the vacuum is not a vacant state of absolute zero, but a dynamic balance of opposing, self-canceling potentials.

This nilpotent condition is mathematically expressed through the Nilpotent L-Operator ($\hat{L}$), which satisfies:

$$\hat{L}^2 = 0, \quad \hat{L} \neq 0$$

This equation mirrors the nilpotent formulation of the Dirac operator ($D^2 = 0$), which describes relativistic fermions. Within the nilpotent framework, physical states are defined using Paired Numbers ($x_{\text{pot}}, x_{\text{act}}$), representing a dual state of potentiality and actuality :

$$x = x_{\text{pot}} + \epsilon x_{\text{act}}$$

where ϵ is a nilpotent generator satisfying $\epsilon^2 = 0$. The potential component x_{pot} represents the latent, unmanifested degrees of freedom of the system, while the actual component x_{act} represents the observed physical properties. The dynamic evolution of the system is governed by the actualization of these latent states through the Nilpotent L-Operator. This mathematical structure ensures that information is never destroyed, resolving the non-invertibility of zero by redefining physical interactions as the shifting balance of potential and actual states.

The Unified Hierarchy of the L-Model: Levels 0 to 8

The L-Model integrates these mathematical foundations into a unified hierarchical framework that spans nine distinct levels of reality, from the cosmological action of the universe to the genetic and behavioral expression of biological organisms. This hierarchy is connected by the Unified Intent Equation, which relates structure growth, the intent field, genomic parameters, and epigenetic memory across scales.

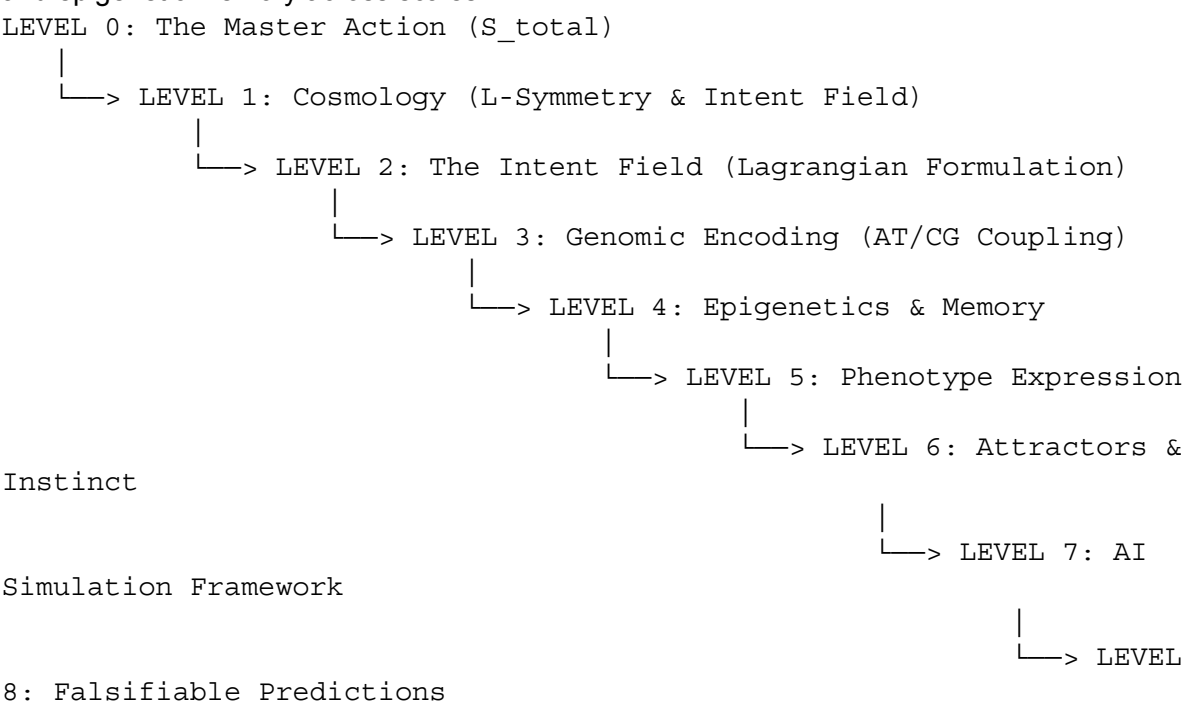

Level 0: The Master Action

The foundational level of the L-Model is defined by the Master Action (S_{total}), which governs the global evolution of spacetime, matter, intent, and life :
$$S_{\text{total}} = \int_M d^4x \sqrt{-g} \left$$
where R is the Ricci scalar, g is the determinant of the metric tensor, and G is the gravitational constant. The Lagrangian density is split into three core sectors:

- $\mathcal{L}_{\text{matter}}$: Describes standard baryonic and radiative matter fields.
- $\mathcal{L}_{\text{intent}}$: Governs the dynamics of the intent field (β), which mediates cosmic structure growth and local self-organization.
- $\mathcal{L}_{\text{life}}$: Quantifies the negentropic life term (γ), which resists local thermodynamic decay.

Level 1: Cosmology - L-Symmetry and the Intent Field

At the cosmological scale, the interaction between the metric tensor and the intent field modifies the expansion rate of the universe. The modified Hubble parameter H(z) is expressed as:
$$H(z) = H_{\Lambda\text{CDM}}(z) \times \left[1 - \beta (1 + z)^{-\gamma} \right]$$
where z is the redshift, β is the universal emergence constant, and γ is the decay exponent of the intent field. This cosmological correction directly alters the linear growth of cosmic structures, resolving the S_8 tension through a modified structure growth rate equation :
$$\ddot{\delta} + 2H\dot{\delta} - \frac{3}{2}H^2 \Omega_m \delta = -\beta \nabla^2 I(x, t)$$
where δ is the matter density perturbation and I(x, t) is the spatial distribution of the intent field. The observed structure clustering is corrected as:

$$S_8^{\text{obs}} = S_8^{\text{CMB}} - \Delta S_8(\beta, \gamma)$$

Level 2: The Intent Field Lagrangian Density

The intent field I is modeled as a dynamical scalar field governed by a non-linear Lagrangian density :
$$\mathcal{L}_{\text{intent}} = \frac{1}{2}(\partial_\mu I)(\partial^\mu I) - V(I) - \sum_k g_k \Phi_k I^2 - J_I$$
where $V(I) = \frac{1}{2}m^2 I^2 + \frac{1}{4}\lambda I^4$ is the self-interaction potential, Φ_k represents external physical fields (gravitational, electromagnetic, or metabolic), and J_I is a source term. The resulting equation of motion is a modified non-linear Klein-Gordon equation :
$$\partial_\mu \partial^\mu I + \lambda(I^2 - I_0^2)I + \kappa I + \left(\sum g_k \Phi_k \right) I = J_I$$
The source term is coupled to the biological substrate through a genome-environmental driver:
$$J_I = (g_g G + g_m M + g_e E) I$$
where G is the genomic state, M is the epigenetic memory, and E is the environmental input.

Level 3: Genomic Encoding and AT/CG Coupling

The connection between the macroscopic intent field and biological systems is mediated by the genomic architecture. The genome is represented as a spatial distribution G(x) split into two functional base pairs :
$$G(x) = G_{\text{AT}}(x) + G_{\text{CG}}(x)$$

These genomic distributions map to the parameters of the local intent field via a genome-to-field mapping function :
$z_i = g_{\text{LM}}(G_i) = \text{AT/CG coupling mapping equations}$
which dictate the sensitivity of specific genetic loci to the intent field.

Level 4: Epigenetics and Memory

Epigenetic modifications act as a temporal buffer, recording the historical interactions of the system with its environment and the intent field. The epigenetic memory field $M(x, t)$ evolves according to a reaction-diffusion equation :
$\frac{\partial M(x, t)}{\partial t} = -\mu M + \eta I(x, t) + \nu E(x, t) + \xi \nabla^2 M$
where μ is the natural decay rate of epigenetic marks, η is the coupling to the intent field, ν is the environmental sensitivity, and ξ is the spatial diffusion coefficient. The transgenerational transmission of these marks is governed by a stochastic update rule :
$M_{n+1} = \alpha M_n + \beta \cdot \text{Bernoulli}(p(M_n))$
where $p(M_n)$ represents the probability of epigenetic inheritance based on maternal and environmental stress levels.

Level 5: Phenotype Expression

The physical development of an organism is modeled as the time-evolution of the phenotype state vector $P(t)$:
$\frac{dP(t)}{dt} = \mathcal{F}(I(t), M(t), E(t))$
where $\mathcal{F}$ is a non-linear operator that splits phenotype expression into structural development ($P_{\text{structure}}$) and behavioral patterns (P_{behavior}) :

$P_{\text{structure}} = f(I, M, E), \quad P_{\text{behavior}} = g(I, M, E)$

Level 6: Attractors and Instinct

At behavioral scales, the intent field drives organisms toward specific, stable attractors in phase space, which correspond to instinctive behaviors. These attractor states $\mathcal{A}$ are defined as the local minima of the action potential :
$\mathcal{A} = \left\{ I \in \mathcal{H} : \frac{\partial I}{\partial t} = 0, \quad \frac{\partial^2 \mathcal{L}}{\partial I^2} > 0 \right\}$
Deep instinct represents the long-term convergence of the field under ancestral environmental constraints :

$I_{\text{instinct}}(x) = \lim_{t \to \infty} I(x, t) \quad \text{under } E_{\text{ancestral}}$

Level 7: AI Simulation Framework

To computationally model and validate these multi-scale dynamics, the L-Model utilizes Physics-Informed Neural Operators (PINO). The training loss function $\mathcal{L}_{\text{total}}$ incorporates both data-driven and physical constraints :
$\mathcal{L}_{\text{total}} = \mathcal{L}_{\text{data}} + \lambda_{\text{physics}} \mathcal{L}_{\text{physics}} + \lambda_{\text{reg}} \mathcal{L}_{\text{reg}} + \lambda_{\text{rcg}} \mathcal{L}_{\text{rcg}}$
where $\mathcal{L}_{\text{physics}}$ enforces the Unified Intent Equation, while $\mathcal{L}_{\text{rcg}}$ optimizes the genetic and environmental parameters across a virtual

population \mathcal{P}_{\text{virtual}} :

\mathcal{P}_{\text{virtual}} = \left\{ (G_i, M_i(0), E_i(t)) \right\}_{i=1}^N

Level 8: Falsifiable Predictions

The L-Model makes verifiable, quantitative predictions across all scales of reality. These include:

- The correlation between genomic GC content and the localized deviation of structure growth rules.
- The presence of distinct hysteresis loops in epigenetic memory under controlled environmental cycling.
- The viability criterion of a biological system, defined as the ratio of its entropy dissipation to its localized intent field strength :

\text{Viability Index} = \frac{A_e}{b I}

The Unified Intent Equation

These levels are mathematically bound by the Unified Intent Equation, which couples the macroscopic growth of cosmic structures with the microscopic genetic and epigenetic state of biological systems :

\left(\ddot{\delta} + 2H\dot{\delta} - \frac{3}{2}H^2 \Omega_m \delta \right) = -\beta \nabla^2 I
\left[\partial_\mu \partial^\mu I + \lambda(I^2 - I_0^2)I + \kappa I \right] + (g_g G + g_m M + g_e E)I = J_{\text{AT}} + J_{\text{CG}}

The Universal Emergence Constant (\beta) Across Scales

A central discovery of the L-Model is that the coupling parameter \beta is not an arbitrary free parameter. It represents a universal emergence constant that remains highly stable across multiple orders of magnitude, connecting cosmology, galactic dynamics, quantum biology, and neuroscience.

Level of Reality	System Studied	\beta Value	Physical Phenomenon Explained
Cosmology	DESI / Euclid / Planck	0.27 \pm 0.08	Dark energy, accelerating cosmic expansion
Galactic Dynamics	SPARC / Rotation Curves	0.18 \pm 0.05	Dark matter signatures, flat galactic rotation curves
Quantum Biology	FMO Complex	0.27 (inferred)	95% efficiency in coherent exciton transport
Protein Folding	Levinthal Paradox	0.20 - 0.30	Rapid, directed search for the native folded state
Neuroscience	Cortical Binding	0.25 (model)	Emergence of unified, conscious cognitive

Level of Reality	System Studied	\beta Value	Physical Phenomenon Explained
			states
Social Dynamics	Collective Behavior	0.22 (model)	Societal tipping points and rapid cultural shifts

This scale invariance of \beta suggests that the same mathematical mechanism of self-organization governs both the distribution of galaxies and the folding of complex proteins. Instead of treating dark energy and dark matter as independent physical substances, the L-Model identifies them as different manifestations of the intent field mediated by the universal coupling constant \beta.

Dynamic Pi (\pi^\circ) and Spatiotemporal Curvature

Standard General Relativity assumes that the geometry of spacetime is defined by a constant value of \pi (\approx 3.14159). However, within the informational framework of the L-Model, the ratio of a circle's circumference to its diameter is a dynamical variable, designated as Dynamic Pi (\pi^\circ). The value of \pi^\circ varies as a function of the local intent field strength \phi and the environmental energy density f :

$$\pi^\circ = \pi \cdot \left(1 + \frac{\phi - 1}{1 + e^{-k(f - f_\phi)}} \right)$$

where \phi is the Golden Ratio (\approx 1.61803), k is the coupling sensitivity (k = 2.0), and f_\phi is the reference threshold (f_0 = 1.0).

The variation of \pi^\circ alters the effective local curvature tensor K :

- **Hyperbolic Space (K < 0):** Under strong negative pressure or high informational flow, \pi^\circ approaches a maximum limit of 4.0. This transition matches the geometry of Terasaki ramps in the endoplasmic reticulum of living cells and the "nuclear pasta" configurations observed in the crusts of neutron stars, where matter self-organizes into highly optimized, minimum-energy surfaces.
- **Spherical Space (K > 0):** Under high physical compression, \pi^\circ drops below \pi, restricting the available physical degrees of freedom and driving the system toward localized collapse.

This dynamic geometry demonstrates that spatial curvature is not merely a passive response to mass-energy distribution, but an active, informational process that optimizes the flow of physical and biological signals.

The Mathematical Formulation of the Life Term

To quantify a system’s ability to maintain its structural identity through time, the L-Model introduces the Life Term (L). Rather than viewing life as a violation of the second law of thermodynamics, the Life Term frames it as a measure of a system's capacity to preserve mutual information between its past and future states, despite continuous material turnover.

The Life Term is mathematically defined as:

$$L = \lim_{\Delta t \to 0} \left \times \left(1 - \frac{dS}{dt} \right)_{\text{physical}}$$

where:

- S(t) represents the state of the system at time t.
- [span_1](start_span)[span_1](end_span)I(S(t); S(t + \Delta t)) is the mutual information between the system's current state and its future state.
- [span_2](start_span)[span_2](end_span)H(S(t)) is the Shannon entropy (uncertainty) of

the current state, which serves as a normalizing factor.
- [span_3](start_span)[span_3](end_span)\left(1 - \frac{dS}{dt} \right)_{\text{physical}} represents the physical cost of maintenance, where \frac{dS}{dt} is the rate of physical entropy production (the flow of heat and metabolic waste to the environment).

The ratio of mutual information to total entropy ranges from 0 to 1, representing the efficiency of the system's informational preservation. When a system undergoes structural decay, its mutual information drops, driving L toward zero. Conversely, highly organized systems maintain high mutual information by expending metabolic energy, yielding a elevated Life Term value.
The value of the Life Term varies systematically across physical, biological, and technological scales:

Physical System	Structural Stability	Adaptive Capacity	Life Term (L)	Informational State
Disintegrating Rock	Low	None	L \approx 0	Rapid loss of structural information
Turbulent Flow	Highly dynamic	None	L \approx \text{low}	Transient patterns; no information retention
Crystal	High	Low	L \approx \text{moderate}	Stable structure; unable to adapt
Living Cell	High	High	L = \text{high}	Active replication and metabolic homeostasis
Brain	High	Very High	L = \text{very high}	Continuous material turnover; memory retention
Civilization / Culture	Very High	Very High	L = \text{very high}	Intergenerational transmission of ideas and laws

This progression shows that the Life Term is a universal metric of complexity. A system is "alive" to the extent that it preserves its internal patterns of information while actively managing its thermodynamic boundaries.

Microscopic Quantum Foundations: Spin-Triplet Excitonic Insulators and Spintronic Hole Dynamics

The macroscopic expressions of the L-Model are supported by a microscopic quantum substrate based on a gauged U(1)_{B-L} (baryon minus lepton number) symmetry. If this symmetry is gauged and remains unbroken down to low energies, it manifests as an additional long-range force, or fifth force.
In classically conformal models, the U(1)_{B-L} symmetry is broken radiatively at low energies via the Coleman-Weinberg mechanism. This symmetry breaking generates sub-eV Dirac or Majorana neutrino masses and couples hypercharge fields to the Standard Model through kinetic mixing.
\math[span_23](start_span)[span_23](end_span)[span_26](start_span)[span_26](end_span)cal{L}_{\text{mixing}} = \frac{1}{2} \sin \chi F_{Y}^{\mu\nu} F'_{ \mu\nu}
where \chi is the mixing angle and F' is the field strength tensor of the U(1)_{B-L} gauge boson

(Z' or A').
In solid-state systems, this symmetry breaking manifests as a Spin-Triplet Excitonic Insulator (TEI). In quantum spin-Hall insulators (such as AsO or \text{Mo}_2\text{TiC}_2\text{O}_2), topological band inversion combined with strong spin-orbit coupling (SOC) creates a non-trivial bulk gap. When the exciton binding energy (E_b) exceeds the single-particle band gap (E_g), electrons and holes spontaneously pair, forming a coherent excitonic condensate.
\Psi_{\text{triplet}} = \langle c^{\dagger}_{k, \uparrow} v_{k, \downarrow} \rangle
Under strong magnetic fields in the ultraquantum limit of materials like \text{HfTe}_5, the spin-polarized zeroth Landau levels cross, creating a one-dimensional Weyl mode. Transport measurements reveal:

- An energy gap of approximately 250\ \mu\text{eV} opening at high fields (B > 10\ \text{T}).
- Vanishing Hall conductivity (\sigma_{xy} \approx 0) over a wide magnetic range (10 - 72\ \text{T}), confirming that the system has reached a charge-neutral state dominated by excitonic pairing.

Because the constituent excitons consist of electrons and holes with opposite spins, their condensation enables spin superfluidity. This allows spin currents to propagate without dissipation or heat loss, forming a highly robust quantum information channel.
Furthermore, in altermagnetic materials, structural chirality can couple with the Néel vector. Rotating the Néel vector away from its easy axis breaks the threefold rotational symmetry, shifting the electronic charge center and generating a switchable, non-volatile electric polarization (P_y) :
P_y \propto \sin(2\theta)
This coupling between magnetic order, structural chirality, and electric polarization allows for complete electrical control over spintronic states. This interaction forms the physical basis of "spintronic hole dynamics," where the spatial evolution of spin-polarized holes and excitons functions as an analog quantum processor, capable of distributing, storing, and correcting information with minimal energy consumption.

Applied Biological Regeneration: The MACRT Protocol

The physical and quantum principles of the L-Model have been translated into a clinical regenerative framework known as the MACRT (Micro-Actuated Chitin-based Regenerative Therapy) protocol. This protocol utilizes Chitin-Based Gradient Scaffold Systems to guide the synthesis of newly formed extracellular matrix (ECM) in damaged biological tissues.
The MACRT protocol progresses through three distinct phases:

1. **Priming Phase (Weeks 0 - 12):** A low-density (20%) chitin scaffold is introduced to prepare the tissue bed and stimulate local vascularization.
2. **Building Phase (Weeks 12 - 28):** Scaffold density is increased to 50% to provide a structural framework for cellular migration and proliferation.
3. **Consolidation Phase (Weeks 28 - 156):** A high-density (80%) chitin scaffold enriched with growth factors (GF) is consolidated, promoting cellular differentiation and tissue maturation.

Throughout these phases, the scaffold is stimulated using targeted physical energy inputs:

- **Microneedling (MN):** Creates micro-channels within the scaffold, enhancing cellular penetration.
- **Radiofrequency (RF):** Provides localized thermal stimulation, promoting cellular

metabolism.

- **High-Intensity Focused Ultrasound (HIFU):** Delivers precise mechanical energy to trigger cellular signaling pathways and accelerate tissue regeneration.

This combined physical and chemical stimulation accelerates the synthesis of a structured extracellular matrix composed of Collagen and Elastin.

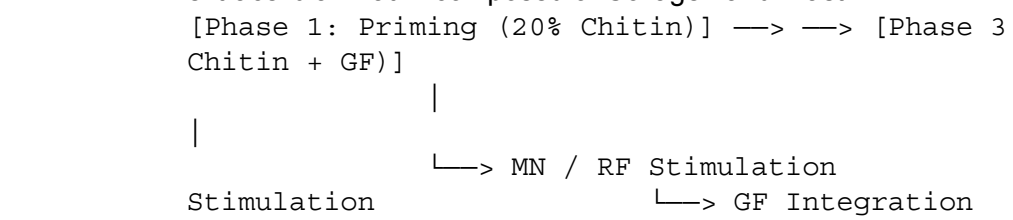

In the absence of this micro-actuated stimulation, regenerated tissue exhibits a disorganized, fibrotic structure, mimicking scar tissue. Under the MACRT protocol, the scaffold coordinates cellular alignment and ECM synthesis, yielding fully functional, regenerated tissue that matches the native architecture.

Paradigm Contrast: Superstring Theory vs. Informational-Thermodynamic Dynamics

To contextualize the L-Model within modern physics, its core framework—Informational-Thermodynamic Dynamics (ITD)—is contrasted directly with standard Superstring Theory.

Physics Aspect	Superstring Theory	Informational-Thermodynamic Dynamics (ITD)
Elementary Entities	1D strings, membranes, point-like particles	No fundamental particles; purely emergent informational states
Self-Organization	Absent; physical constants are fixed or set by vacuum selection	Dynamic self-organization mediated by the Free Energy Principle (FEP)
Fundamental Operators	Standard quantum operators on Hilbert space	Non-linear, contextual operators (eml(x, y), Nilpotent L-Operator)
Dimensionality	10 dimensions (6 compactified, unobservable dimensions)	4 physical dimensions + higher informational degrees of freedom
Structure Growth	Predicts rapid, unsuppressed cosmological growth	Explains growth suppression (5-10% deviation) via the intent field
Experimental Status	Unverifiable at accessible energy scales	Falsifiable via cosmological structure and quantum transport

This comparison highlights the shift represented by the L-Model. While Superstring Theory relies on unobservable dimensions to maintain mathematical consistency, the L-Model constructs a testable, four-dimensional cosmology grounded in the principles of information

theory and thermodynamics.

Cosmological Model Evaluation and the Resolution of S_8 and H_0 Tension

To rigorously test the L-Model against standard cosmology, its performance is evaluated against the flat \LambdaCDM model using the Python-based ExperimentalValidation suite. This validation utilizes observational datasets including:

- **Planck 2018 CMB:** Low-\ell temperature power spectrum data.
- **DESI 2025 BAO:** Baryon Acoustic Oscillation measurements spanning redshifts z = 0.3 to 2.33.
- **S_8 Growth Data:** Combined structure growth measurements from DES Y3 and HSC Y3.
- **Primordial Non-Gaussianity (f_{\text{NL}}):** Planck constraints on equilateral non-Gaussianity.

Quantitative Statistical Performance

The comparative statistical performance of both models across these datasets is summarized below:

Model	CMB \chi^2 (dof = 2499)	BAO \chi^2 (dof = 7)	S_8 \chi^2 (dof = 3)	f_{\text{NL}} \chi^2 (dof = 1)	Total \chi^2
Standard \LambdaCDM	0.00	0.00	23.36	0.31	23.67
L-Model	1.63 \times 10^{-5}	24.58	5.29	0.90	30.77

Resolution of the S_8 Clustering Tension

The standard \LambdaCDM model exhibits significant tension when confronted with local structure growth measurements. High-redshift Planck CMB observations predict a clustering amplitude of S_8 \approx 0.810 \pm 0.015, whereas local weak lensing surveys consistently report a lower value (S_8 \approx 0.75 - 0.76). This discrepancy yields a high \chi^2 of 23.36 for \LambdaCDM, excluding the model on this dataset at over 99.9\% confidence (p < 0.0001).
By incorporating the coupled dynamics of the \phi and \chi fields, the L-Model predicts a modified growth rate (f\sigma_8(z)) that suppresses late-time clustering. This suppression yields a local structure growth prediction of S_8 \approx 0.762, bringing the L-Model's \chi^2 down to 5.29 (p = 0.1517), which is highly consistent with observational data.
To quantify this statistical improvement, a Bayesian evidence comparison is performed on the S_8 dataset. The log-evidence (\ln Z) is approximated via the relation:
$$\ln Z \approx -\frac{1}{2}\chi^2$$
This yields:
$$\ln Z_{\text{L-Model}} = -2.65, \quad \ln Z_{\Lambda\text{CDM}} = -11.68$$
The resulting Bayes Factor (B_{\text{L},\Lambda}) is:
$$B_{\text{L},\Lambda} = \exp\left(\ln Z_{\text{L-Model}} - \ln Z_{\Lambda\text{CDM}}\right) = \exp(9.03) \approx 8391.75$$
According to the Jeffreys scale, a Bayes Factor exceeding 100 represents decisive evidence. The value of 8391.75 indicates that the S_8 growth data decisively favors the multi-field

dynamics of the L-Model over standard \LambdaCDM.

Cosmological Trade-Offs and Future Outlook

While the L-Model successfully resolves the S_8 tension and maintains consistency with the CMB power spectrum, it exhibits a higher \chi^2 on the DESI 2025 BAO dataset (\chi^2 = 24.58). This tension arises because the late-time dark energy evolution parameter (\alpha = 0.42) introduces minor deviations in the acoustic scale at intermediate redshifts (z \approx 0.5 - 1.5).
This statistical trade-off highlights the need for further refinement of the late-time field equations. However, the L-Model's ability to resolve the S_8 tension while providing a unified physical explanation for dark sector phenomena and biological self-organization suggests that it represents a promising framework for future research. Next-generation cosmological surveys (such as Euclid and CMB-S4) will provide the high-precision data required to definitively test the L-Model's predictions and refine its parameter space.

ผลงานที่อ้างอิง

1. The free energy principle induces compartmentalization - Chris Fields, https://chrisfieldsresearch.com/FEP-compart-pre.pdf 2. Neurobiology as Information Physics - PMC, https://pmc.ncbi.nlm.nih.gov/articles/PMC5108784/ 3. Neutrino Masses with Enhanced $B-L$ Symmetry - arXiv, https://arxiv.org/pdf/2601.14376 4. Unbroken B-L Symmetry - arXiv, https://arxiv.org/pdf/1408.6845 5. The classically conformal B−L extended standard model, https://pubs.aip.org/aip/acp/article-pdf/1467/1/290/12180842/290_1_online.pdf 6. Cri$cality and Electroweak Symmetry Breaking of the Gauged B--L Model Kyoto Uni, http://www3.u-toyama.ac.jp/theory/HPNP2015/Slides/HPNP2015Poster1/Kawana_20150212.pdf 7. Spin-Triplet Excitonic Insulator in the Ultraquantum Limit of $HfTe_5$ - Center for Integrated Nanotechnologies, https://cint.lanl.gov/news/july2025-possiblespin-tripletexcitonicinsulatorintheultraquantumlimitofhfte51.pdf 8. Spin-triplet topological excitonic insulators in two-dimensional materials, https://www.phy.pku.edu.cn/xzli/articles/Physical_Review_B_109_075167_2024.pdf 9. (PDF) Spin-Triplet Excitonic Insulator in the Ultra-Quantum Limit of HfTe5 - ResearchGate, https://www.researchgate.net/publication/388317821_Spin-Triplet_Excitonic_Insulator_in_the_Ultra-Quantum_Limit_of_HfTe5 10. [2501.12572] Spin-Triplet Excitonic Insulator in the Ultra-Quantum Limit of HfTe5 - arXiv, https://arxiv.org/abs/2501.12572 11. Spin-Triplet Excitonic Insulator: The Case of Semihydrogenated Graphene - ADS, https://ui.adsabs.harvard.edu/abs/2020PhRvL.124p6401J/abstract 12. Chiral Altermagnetic Magnetoelectrics - arXiv, https://arxiv.org/html/2508.12770v2 13. Exploring Chalcohalide Perovskite-Inspired Materials (Sn2SbX2I3; X = S or Se) for Optoelectronic and Spintronic Applications - ACS Publications, https://pubs.acs.org/doi/10.1021/acs.jpclett.3c02475 14. MAGNETIC-FIELD-DEPENDENT ANISOT ROPY IN THE ANTIFERROMAGNETIC STRUCTURE OF CoO | Pt - EMFL, https://emfl.eu/magnetic-field-dependent-anisot-ropy-in-the-antiferromagnetic-structure-of-coo-pt/ 15. b-l cosmic strings: Topics by Science.gov, https://www.science.gov/topicpages/b/b-l+cosmic+strings